International Journal of Modern Physics B, Vol. 8, No. 3 (1994) 207–235

FRACTAL AND DYNAMICAL PROPERTIES OF THE KICKED HARPER MODEL

R. ARTUSO and G. CASATI
**Università di Milano, Sede di Como, Via Castelnuovo 7, I-22100 Como*
and
I.N.F.N. Sezione di Milano

F. BORGONOVI and L. REBUZZINI
Dipartimento di Fisica Nucleare e Teorica, Università di Pavia, Via Bassi 6, I-27100 Pavia
and
†I.N.F.N. Sezione di Pavia

and

I. GUARNERI*, †

Received 10 July 1993

We review recent work on the so-called kicked Harper model, which can be viewed either as a model system in the framework of quantum chaos, or as a pulsed version of the Harper model, which has been thoroughly investigated in the context of magnetic field effects in solid state physics. In particular we describe its rich phase diagram, by means of both dynamical methods and multifractal analysis of the spectrum.

1. Introduction

Harper's equation was introduced in 1955[1] as an approximate model for electrons in a two-dimensional crystal in the presence of a perpendicular magnetic field. Its derivation involves different drastic approximations, as it takes into account a single Bloch band, with a tight binding energy form, from which the effective Hamiltonian is derived by Peierls' substitution. This amounts in converting $\hbar\underline{\mathbf{k}}$ appearing in the explicit expression of the Bloch energy function with no field, into the operator $\underline{\mathbf{p}} - e/c\underline{\mathbf{A}}$, thus turning the starting function into the effective Hamilton operator of the system once the field is turned on (further details and references can be found in Ref. 2).

The eigenvalue (difference) equation is written

$$\frac{1}{2}K\left(\phi_{n+1} + \phi_{n-1}\right) + L\cos\left(2\pi\sigma n + \theta\right)\phi_n = \epsilon\phi_n \tag{1.1}$$

where the modulation parameter σ gives the ratio of flux through a lattice cell to one flux quantum.

The original derivation (1.1) has been found to provide an approximate description of many other physical systems,[3] and fresh interest in the problem has also been prompted in the framework of the quantum Hall effect.[4] The spectrum of (1.1) has several peculiar properties: first of all Azbel[5] observed that an irrational value of σ may generate a Cantor-set spectrum, while if $\sigma = p/q$ the system is periodic with period q, so we have Bloch eigenfunctions and a spectrum consisting of q bands. One of the most striking features of the model is a duality property[6]: that is if we perform the transformation

$$g_m = \sum_{n=-\infty}^{\infty} \phi_n \, e^{-in(2\pi\sigma m+\theta)} \, e^{-im\theta}$$

then the set of $\{g_m\}$ satisfies

$$\frac{1}{2}K\,(g_{n+1} + g_{n-1}) + L\cos(2\pi\sigma n + \theta)\, g_n = \epsilon g_n$$

which is the same as (1.1) but with the role of K and L interchanged. By using this duality property and Thouless' formula[7] Aubry and André gave arguments showing that a metal–insulator transition occurs at $K = L$.

The nature of the spectrum of (1.1) has been widely investigated in the mathematical literature (see Refs. 8 and 9 for the relevant results and references). If the modulation parameter σ is irrational, the associated almost periodic Schrödinger operator presents peculiar features, considered pathologies from a "conventional" point of view, like possible occurrence of dense point spectrum, singular continuous spectrum and absolutely continuous spectrum with non trivial scaling properties.[10] In particular spectral properties of (1.1) depend crucially on number theoretical properties of the (irrational) modulation parameter σ: quite different behaviors are expected depending on whether σ has good diophantine properties or is a Liouville number (that is approximated very badly or very well by rational numbers). For strongly irrational values of σ (like $\sigma = \rho_{\mathrm{GM}}^{-1} = (\sqrt{5}-1)/2$) it is believed that for $K < L$ all states are exponentially localized, so, by duality, for $K > L$ all states are extended, while the spectrum is singular continuous with critical states at the self-dual point $K = L$. This has been checked by scaling analysis of the spectrum by Kohmoto and Tang,[11] by a method we will comment upon and employ in later sections (for a useful review, which contains related work for other tight binding models see Ref. 12).

A question of fundamental import is tied to how spectral properties affect dynamical behavior: while extended states and localized states lead respectively to ballistic spreading and no spreading at all in the long time limit (at least this is the heuristic expectation, not fully supported by rigorous results), it is not *a priori* clear what should happen in the critical case. This question was addressed in Ref. 13, and the spreading of the wave packet was found to be given by $\langle \Delta x_t^2 \rangle \sim t^{\alpha}$ with α close to one (which would correspond to normal diffusion). In fact these

authors report $\alpha/2 = 0.485$ for golden mean modulation, and very close exponents for other quadratic irrationals: moreover, on the basis of former work on the Fibonacci quasicrystal[14] they compare $\alpha/2$ with the spectrum of scalings studied by Tang and Kohmoto,[11] noticing that $\alpha/2$ is very near to the scaling index for which $f(\alpha)$ reaches its maximum.[a] The same exponent ($\alpha/2$) was related to the Hausdorff dimension of the spectrum in Refs. 15 and 16, as well as to some sort of power-law level statistics (apparently first observed in Ref. 17). We remark that a rigorous bound was established by Guarneri,[18] relating the rate of spreading of wave packets to the information dimension D_I of the spectrum ($\alpha/2 \geq D_I$), in a quite general framework of discrete unitary group evolution on a one-dimensional lattice: this type of bound has been confirmed and generalized.[19] Since information dimension is bound from above by Hausdorff dimension, this bound is compatible with the numerical findings and heuristic arguments quoted above. We add as a further remark that through scaling arguments and numerical calculations[20] (based upon a derivation — using perturbation theory — of some clustering rules proposed by Hofstadter[21]) it has been conjectured that $D_{\mathrm{H}} = 0.5$ for typical modulation parameter σ.

We may think of the kicked Harper model as a sort of modified Harper model, in which the field is delta pulsed, thus being described by the (time-dependent) Hamiltonian

$$\hat{H} = L\cos(\hat{p}) + K\cos(\hat{x})\delta_1(t) \tag{1.2}$$

where

$$\delta_1(t) = \sum_{n=-\infty}^{\infty} \delta(t-n) \quad \text{and} \quad \hat{p} = -i\hbar\frac{\partial}{\partial x}$$

and where the modulation parameter is now the effective Planck constant $\hbar$ (which thus plays the role of $2\pi\sigma$). To our knowledge the first proposal to study such a system came in a paper[22] where some Schrödinger-type equations were derived in connection to time–dependent velocity fields characterized by chaotic advection properties. The system was analyzed in Ref. 23 to investigate relationships between topological invariants (Chern number of the band) and nodal properties of the eigenfunctions (which are claimed to be connected to phase–space localization), along the lines of Thouless *et al.*'s approach to quantized Hall conductance.[4] The kicked Harper model was investigated by Lima and Shepelyansky,[24] who analyzed its dynamical features (spreading of an initial wave packet), motivated by the well-known results[25] for the kicked rotator, characterized by the quantum suppression of classical chaotic diffusion. The operator (1.2) can be derived upon standard quantization of the classical two-dimensional area preserving map

$$p_{n+1} = p_n + K\sin(x_n) \qquad x_{n+1} = x_n - L\sin(p_{n+1}) \pmod{(2\pi)} . \tag{1.3}$$

[a]We point out that, as we will comment upon in the following, the $f(\alpha)$ calculated by Kohmoto and Tang does not contain information on the "dynamical" spectral measure, so one has to be careful in comparing dynamical exponents with scaling indices referring to it (except D_{H}).

This map was introduced[26] to investigate the dynamics of classical particles in a static magnetic field and in the field of a wave packet which is propagating across the magnetic field. The investigation of quantum behavior[24] (for K and L yielding chaotic behavior in the classical map, and strongly irrational values of $\hbar$) revealed a rich variety of dynamical behavior (in particular dynamical localization is present only in a fraction of the parameters' space), symmetric pairs ($K = L$) giving rise to quantum diffusion, ($K > L$) pairs originating ballistic spreading and dynamical localization for ($K < L$) values (even though departures from this general picture were mentioned, see also Ref. 27). The overall parameter space picture was confirmed by Geisel, Ketzmerick and Petschel, who claimed that the kicked Harper model was characterized by the same critical exponents of Harper's model: both as regards the spreading of the wave packet and small scale level statistics[28] and in the exponents ruling power-law decay of autocorrelation functions[29] (differences, due to chaotic classical dynamics, appearing only in transients).

We investigated the model in much detail, motivated both by the striking differences reported in the quantum behavior when compared with other quantized area preserving maps, and to pursue if really the kicking did not change the "universality class" of the model. We found a non-trivial behavior along the symmetric line ($K = L$),[30] indicating a richer dynamics than formerly supposed, as well as a complicated structure of the phase diagram.[31] It is to be remarked that however, kicked Harper model has much in common with the usual Harper model duality properties,[33] and this gives strong mathematical support for the existence of extended quasienergy eigenstates in some region of the (K, L) plane. As a matter of fact, the existence of delocalized regimes has been rigorously proved for a class of models defined by a Hamiltonian like (1.2), but with a generic analytic function in place of the cosinus.[33] A brief account of such results will be given in Sec. 6.

This review is intended to present the main points of our investigations, both as regards dynamical analysis and thermodynamics' approach to spectral properties.[11,32] Before going into details about our methods and results we mention that other features of the kicked Harper model have been investigated in the literature (see e.g. Refs. 35 and 36).

2. The Model and Possible Ways to Investigate its Dynamical Behavior

We thus start from the classical map (1.3), which we imagine acting on the cylinder (the x-coordinate is taken modulo 2π: this angle will be denoted by θ in the following). A large fraction of its phase diagram is characterized by chaotic diffusion: in this respect the map behaves differently from the classical standard map, in which the transition to unbounded chaos follows a critical transition to chaos for golden mean torus,[37] as here (for instance in the symmetric $K = L$ case) diffusion is supported along a stochastic web which is built upon destruction of a lattice-like separatrices net.[26]

The quantum version of the model is obtained by canonical quantization[25] of (1.3), and leads to the Floquet operator

$$\hat{U}_{L,K} = \exp\left(-i\frac{L}{\hbar}\cos(\hbar\hat{n})\right)\exp\left(-i\frac{K}{\hbar}\cos(\theta)\right) \tag{2.1}$$

where $\hat{n} = -i\partial/\partial\theta$ and periodic boundary conditions are assumed. This operator corresponds to the unitary evolution over a unit time-step: the corresponding propagator in the standard Harper model is recovered via the limit $\lim_{t\to\infty}\hat{U}_{Lt^{-1},Kt^{-1}}$. The quasienergy spectrum is determined by the eigenvalue equation

$$\hat{U}_{L,K}\psi_\omega = e^{-i\omega}\psi_\omega$$

and depends crucially on the number theoretic properties of $\hbar$, which, we recall, plays in this context the role of the incommensurability parameter. The eigenvalue equation is conveniently expressed in the Fourier (momentum) basis

$$\psi_\omega(\theta) = \sum_{m=-\infty}^{\infty} e^{im\theta}\,\phi_m \qquad \phi_m = (2\pi)^{-1}\int_0^{2\pi} d\theta\,\psi_\omega(\theta)e^{im\theta}\,.$$

In this representation the eigenvalue equation becomes

$$e^{-i\omega}\phi_m = \sum_{m'} U_{m,m'}\phi_{m'} \tag{2.2}$$

where

$$U_{m,m'} = (2\pi)^{-1}e^{-i\frac{L}{\hbar}\cos(\hbar m)}\int_0^{2\pi} dx\,e^{i(m'-m)x}e^{-i\frac{K}{\hbar}\cos(x)}\,.$$

By employing the Jacobi–Anger expansion this can be written as

$$U_{m,m'} = e^{-i\frac{L}{\hbar}\cos(\hbar m)}i^{m-m'}J_{m-m'}\left(-\frac{K}{\hbar}\right)$$

where the decay properties of the diagonal elements are expressed in a more transparent way: in particular hopping terms that couple rather distant sites may be relevant when the argument of the Bessel function is large. The eigenvalue equation presents remarkable features when $\hbar = 2\pi p/q$. As a matter of fact in this case $U_{m+q\,m'+q} = U_{m,m'}$ and we have Bloch eigenfunctions $\phi_{s+q\cdot l} = e^{-ial}\phi_s$ $s = 1, \ldots, q$; $l \in \mathbf{Z}$ $a \in [0, 1)$ and (2.2) reduces to the matrix equation[38]

$$[U(a)]_{s,s'}\,\phi(a)_{s'} = \phi(a)_s\,e^{-i\omega(a)}$$

where the unitary operator

$$[U(a)]_{s,s'} = \frac{1}{q}\sum_{j=1}^{q} \exp\left(i\left(\frac{2\pi}{q}(j+a)\right)(s'-s)\right) \exp\left(-i\frac{K}{\hbar}\cos\left(\frac{2\pi}{q}(j+a)\right)\right)$$
$$\times \exp\left(-i\frac{L}{2\hbar}(\cos(\hbar s)+\cos(\hbar s'))\right) \tag{2.3}$$

determines the eigenstates on a torus of length q. The one-period evolution operator (2.1) is the product of two non-commuting exponentials: the K-part is diagonal in the phase representation, while the L-part is diagonal in the momentum representation: this makes it convenient to follow time evolution numerically by fast Fourier transform from one basis to the other (so that the only remaining operations are multiplications). The reliability checks on such an algorithm are performed by controlling that the results we obtain are not influenced by the (finite) size of the Fourier basis we work with. We usually used a Fourier basis of 2^{17} unperturbed eigenstates, which proved to give reliable results for time series up to $3\cdot 10^5$ kicks, by taking initial states of various shapes initially localized around the zero-component of momentum.

The dynamical information we get from each run amounts to the autocorrelation function $\{\langle\psi_0|\hat{U}^m_{L,K}\psi_0\rangle\}$ and the probability distribution over unperturbed eigenstates $p_m(k) = \left|\langle\phi_k|\hat{U}^m_{L,K}\psi_0\rangle\right|^2$. From this distribution we can reconstruct time behavior for different moments (we always have $\sum_k p_m(k)\cdot k = 0$)

$$\sigma_q(m) = \sum_k |k|^q p_m(k)\ . \tag{2.4}$$

In particular the spreading of the wave packet is governed by the variance $\sigma_2(m)$. In the case of the kicked rotator[25] $\sigma_2(m)$ is asymptotically bounded, in agreement with the fact that this model should be characterized by a pure point spectrum.[39] This is just one of the remarkable connections between dynamical properties and spectral analysis, an argument we already mentioned and that will be commented upon in later sections. It also plays a role in the discussion of correlations: in this respect the quantity we will investigate will be the integrated, or time-averaged, correlation function

$$C_{\rm int}(m) = \frac{1}{m}\sum_{k=0}^{m-1}\left|\langle\psi_0|\hat{U}^k_{L,K}\psi_0\rangle\right|^2\ . \tag{2.5}$$

This quantity is directly linked to the spectral measure, as the autocorrelation function is the Fourier transform of the latter

$$C(m) = \langle\psi_0\,|\,\hat{U}^k_{L,K}\,\psi_0\rangle = \int_0^1 d\mu_{\psi_0}(x)\,e^{-2\pi i x k}\ .$$

In particular a rigorous criterion for the existence of a pure point component of the spectral measure is the convergence of (2.5) to a non-zero limit as $m \mapsto \infty$. In the case of purely continuous spectrum a power-law behavior is expected for singular continuous or recurrent absolutely continuous spectrum,[10] and moreover the exponent δ ruling this decay ($C_{\text{int}}(m) \sim m^{-\delta}$) should coincide with the correlation dimension of the fractal measure.[29] We add as a remark that different possible decays of autocorrelation functions have been observed in a simple quasiperiodic system.[40]

3. Scaling Analysis of the Spectrum and the Thermodynamic Formalism

We have already pointed out that a careful consideration of the spectrum is of outmost importance in this context, and was pioneered by Kohmoto and Tang[11] in the analysis of Harper's equation. Before reviewing the version of the thermodynamic formalism we will employ in the following, a comment is in order. We will mainly use a purely "metric" approach to the limiting spectrum, that is we will not take into account the fact that, once we select an initial wave packet a spectral measure is determined on the spectrum itself. This is dictated by the hierarchical approach we will put forward, and prevents a quantitative comparison between spectral indices and dynamical exponents.[41] A multifractal analysis of the spectral measure requires different techniques, which are presently under active investigation.[42]

The main idea underlying the Kohmoto–Tang approach is to build up a sequence of rational (p_n/q_n) approximations to the incommensurability parameter $\hbar/2\pi$. In particular we consider $\hbar/2\pi$ with good diophantine properties (typically corresponding to quadratic irrationals),[43] the sequence p_n/q_n being determined by successive truncations of the continued fraction expansion of $\hbar/2\pi$. This represents an optimal choice of rational approximations,[44] with exponentially increasing q_n (for quadratic irrationals), $q_n \sim a^n$. To each p_n/q_n there corresponds a periodic system, whose spectrum consists of q_n bands whose length we denote by $w_{i(n)}$, which we can calculate by diagonalizing (2.3) for all values of the Bloch phase a (see Fig. 1). This procedure can be viewed like a sequence of more and more refined coverings of the spectrum, whose scaling properties are then studied in the framework of the thermodynamic formalism[45]: we will now recall the introduction of the key quantities, following the notation in Ref. 46.

At each level n of the hierarchical sequence of coverings $(w_{i(n)}\, i(n) = 1, \ldots, q_n)$ one can associate the "partition sum"

$$Z_n(\tau) = \sum_{i=1}^{q_n} w_{i(n)}^{-\tau} \tag{3.1}$$

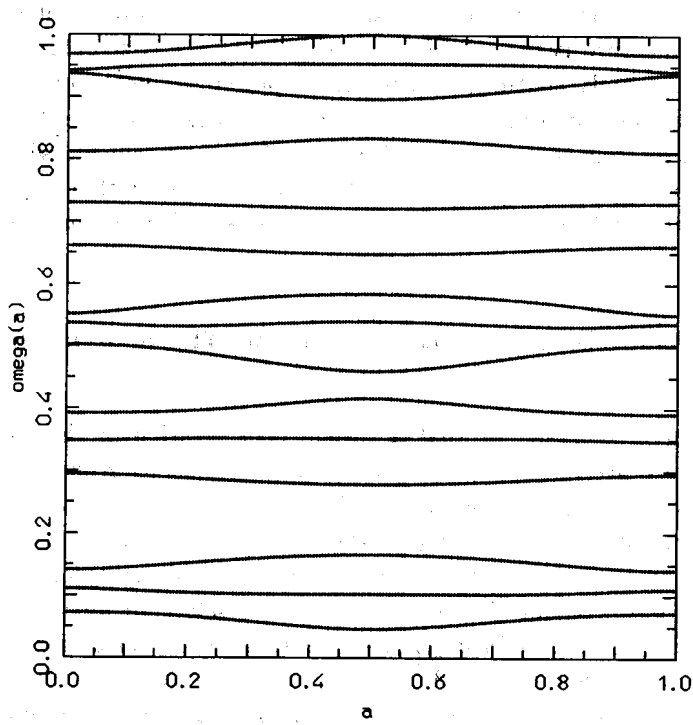

Fig. 1. Quasienergy eigenvalues as a function of the Bloch phase a ($K = L = 5$ $\hbar = 2\pi \cdot 2/15$).

where the weighting parameter τ (formally analogous to an inverse temperature) is allowed to vary over the whole real axis. The role of τ is to probe different sizes of the covering intervals: as $\tau \to \infty$ the sum (which will diverge) is dominated by the thinnest intervals, while at the opposite limit the behavior is dominated by the fattest $w_{i(n)}$. The relevance of (3.1) in accounting for scaling properties is easily appreciated if one recalls that the critical value of τ, τ_c such that

$$Z_n(\tau) \to 0 \, (n \to \infty) \quad \tau < \tau_c$$

$$Z_n(\tau) \to \infty \, (n \to \infty) \quad \tau > \tau_c$$

determines the Hausdorff dimension[47] of the set ($D_H = -\tau_c$). The scaling properties will be encoded in the free energy $g(\tau)$, defined in the thermodynamic limit

$$g(\tau) = \lim_{n \to \infty} g_n(\tau)$$

where finite size approximations are determined by

$$Z_n(\tau) = q_n^{g_n(\tau)} \tag{3.2}$$

$g(\tau)$ is a monotonically increasing function of τ, and its zero determines the Hausdorff dimension $g(-D_H) = 0$, while it is easy to check that $g(0) = 1$. Thus for a homogeneous fractal set (like the usual middle-third Cantor set) $g(\tau)$ is a straight line with slope D_H^{-1}. In general the first derivative of $g(\tau)$ will span the whole set of scales characterizing the set. If we define scaling exponents $\{\mu_{i(n)}\}$ by

$$\mu_{i(n)} = -\frac{\log w_{i(n)}}{\log q_n} \tag{3.3}$$

and rewrite

$$Z_n(\tau) = \sum_{i=1}^{q_n} q_n^{\tau\mu_{i(n)}}$$

it is easy to see that

$$g'(\tau) = \mu(\tau) = \lim_{n\to\infty} \frac{\sum_i^{(n)} \mu_{i(n)} q_n^{\mu_{i(n)}\tau}}{\sum_i^{(n)} q_n^{\mu_{i(n)}\tau}}$$

so that $\mu(\tau)$ gives the scaling exponent dominating the partition sum for weighting factor τ. A useful function accounting for the distribution of scaling exponents is given by the scaling spectrum $s(\mu)$, which is defined once the sum (3.1) is reordered by increasing length size

$$s(\mu) = \lim_{n\to\infty} s_n(\mu) \quad Z_n(\tau) = \int_{\mu_{\min}}^{\mu_{\max}} d\mu\, q_n^{s_n(\mu)+\mu\tau} \tag{3.4}$$

where $q_n^{s_n(\mu)} d\mu$ gives the number of coverings (at the nth step of the hierarchical procedure) whose scaling exponent is within μ and $\mu + d\mu$. The scaling spectrum $s(\mu)$ is a highly irregular function of μ for finite n: in practice one evaluates $g_n(\tau)$ and replaces $s(\mu)$ by its convex envelope $S(\mu)$, evaluated in the thermodynamic limit saddle point evaluation of (3.4).

$$q_n^{g_n(\tau)} = C(n) \left[-\frac{2\pi \log q_n}{S_n''(\tau)}\right]^{1/2} q_n^{(S_n(\overline{\mu})+\tau\overline{\mu})}$$

where $\overline{\mu}(\tau)$ is the solution of the extremum condition

$$\left.\frac{dS_n(\tau)}{d\mu}\right|_{\overline{\mu}} = -\tau\ .$$

The distinction between the scaling spectrum and its convex envelope is a crucial tool in diagnosing phase transitions (a concavity in $s(\mu)$ signals a first order phase transition).[46,48] The inverse function $\tau(q)$ gives the spectrum of generalized dimensions D_q (Halsey *et al.* in Refs. 45 and 49), through the relation $\tau(q) = (q-1)D_q$. Again we remark that the only generalized dimension of the spectral measure coinciding with the set we calculate along the former prescription is the Hausdorff

dimension, which is the only one which is insensitive to the choice of probability measure attached upon the set.

In terms of this formalism the results obtained for Harper's equation by Kohmoto and Tang[11] (in full agreement with the discussion in terms of duality properties[6]) may be summarized as follows. In the localization regime no scaling behavior is observed, as bands shrink faster than exponentially (we remark that this is also true for the kicked rotator[50]). In the extended regime the scaling spectrum collapses to two points ($s = 1$ for $\mu = 1$, and $s = 0$ for $\mu = 2$), the first giving the indication of an absolutely continuous spectrum, while the other is a remnant of Van Hove singularities. The critical case is characterized by a non-trivial scaling spectrum, with $D_H = 0.5$ and scaling exponents strictly larger than one: this should correspond to a purely singular continuous spectrum. Single scaling exponents have been thoroughly studied for a number of other tight binding models,[12] while, as we will illustrate in the following, features of the scaling spectrum indicating mixed spectra were commented upon in Ref. 32. The extended case analysis thus provides a simple example of a phase transition[51]: we shall see that the kicked Harper model will provide examples of subtler phase transitions, similar, in a sense, to the one that characterizes the structure of Hénon's attractor.[52]

4. Behavior Along the Critical Line

The first parameter region we investigated[30] is the critical line $K = L$. We considered incommensurability parameter $\hbar/2\pi$ of the form $1/(m + \rho_{GM})$, in order to vary the parameter $\gamma = K/\hbar$ either by changing K or $\hbar$, but leaving the number theoretic properties of the modulation unaltered. The first result we get (in agreement with Refs. 24 and 28) is that the spreading of the wave packet is unbounded, and well-described, after an initial transient, by a law of the form $\sigma_2(m) \sim m^\chi$. In Refs. 15 and 16 a general relation was proposed, of the form $\chi = 2D_H$, moreover[15,28] for either kicked or unkicked Harper D_H was conjectured to be 1/2. While for parameters values approaching the Harper's equation limit ($K/\hbar \to 0$) we found this to hold, for higher values of $K/\hbar$ we discovered examples of anomalous (enhanced) diffusion: for instance (see Fig. 2) for $K = L = 5$ and $\hbar/2\pi = (18 + \rho_{GM})^{-1}$ the growth exponent χ takes the value 1.42. This strongly suggests that the kicked Harper model is characterized by a richer behavior than the Harper model, and at the same time prompts for a more detailed investigation of the proposed relation between the diffusion exponent and Hausdorff dimension of the spectrum. This quantity is calculated following the hierarchical approach illustrated in the former section, for a selection of parameters' values. Once the band widths $\{w_{i(n)}\}$ have been calculated for a subsequence of hierarchical indices n (each corresponding to a periodic approximation $\hbar/2\pi = p_n/q_n$), nth order estimates of D_H are calculated by solving

$$\sum_{i=1}^{q_n} w_{i(n)}^{D_n} = 1 \, .$$

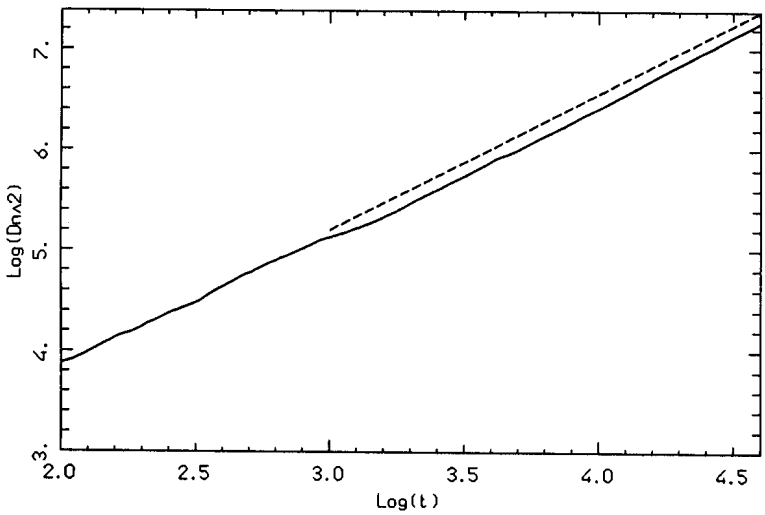

Fig. 2. $\log \sigma_2(m)$ vs. $\log t$ for $K = L = 5$ $\hbar = 2\pi/(18 + \rho_{GM})$ (full line). The dashed line has a slope $2D_H = 1.4$.

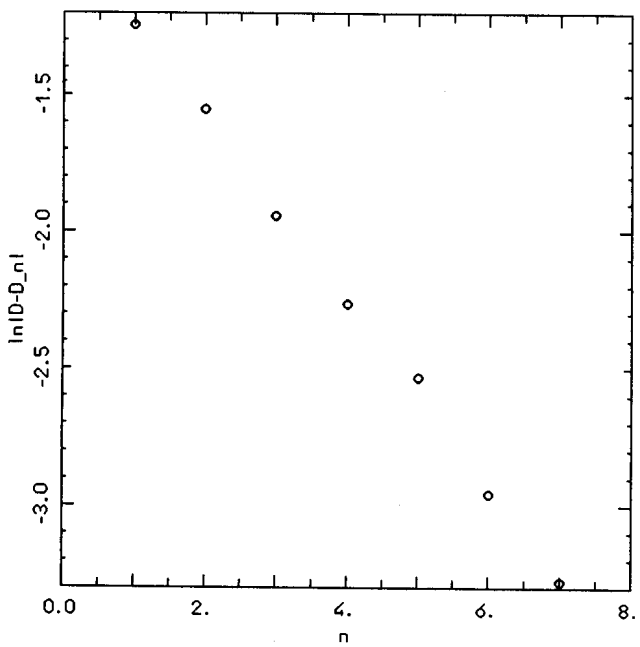

Fig. 3. $\log |D_n - D_H|$ vs. n for $K = L = 5$ $\hbar = 2\pi/(18 + \rho_{GM})$.

The $\{D_n\}$ sequence is generally found to converge geometrically (see Fig. 3), which allows one to estimate D_H within a small percentage. While generally D_H tends to increase for higher values of $K/\hbar$ we do not have evidence of any scaling property

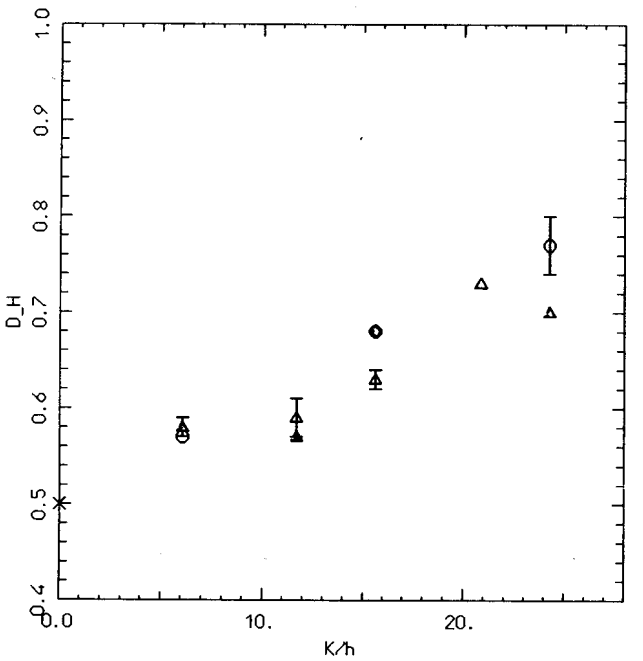

Fig. 4. Hausdorff dimension estimates (o $\hbar = 2\pi/(6+\rho_{GM})$, • $\hbar = 2\pi/(18+\rho_{GM})$, Δ $\hbar = 2\pi/(1+\rho_{GM})$, ▲ $\hbar = 2\pi/(3+\rho_{GM})$). × indicates the Harper limit. A few error bars are reported.

in terms of this parameter (see Fig. 4). Within the set of parameters investigated we observed discrepancies between $2D_H$ and the diffusion exponent χ (see Fig. 5), which in these cases gets a smaller value than $2D_H$. This is in agreement with recent theoretical bounds.[53] While Hausdorff dimension calculations exhibit good convergence, this does not hold for the whole range of thermodynamical functions: in particular it seems that a maximal scaling index is not defined. This can be appreciated by plotting finite order estimates for the mean scaling exponent $\mu(\tau)$ (Fig. 6), and it is due to bandwidths shrinking faster than exponentially. On the basis of tight binding[11,12] and kicked rotator[50] models this may be interpreted as an effect of a portion of point component in the spectrum: its occurrence seems typical (see Table 1). As we anticipated this somehow resembles what one observes in the thermodynamic analysis of the Hénon strange attractor,[52] where a phase is dominated by longer and longer orbits which come closer and closer to turnbacks, making only averages dominated by the "hyperbolic" phase meaningful. In our case the stable phase seems to be associated with the negative τ region, and this confirms the reliability of Hausdorff dimension calculations. The unstable phase seems dominated by very few thin intervals, as one can see by a comparison of the scaling spectrum $s_n(\mu)$ (obtained by statistics on different $\{w_{i(n)}\}$ sets) and its convex envelope $S_n(\mu)$ (coming from a Legendre transform of the free energy):

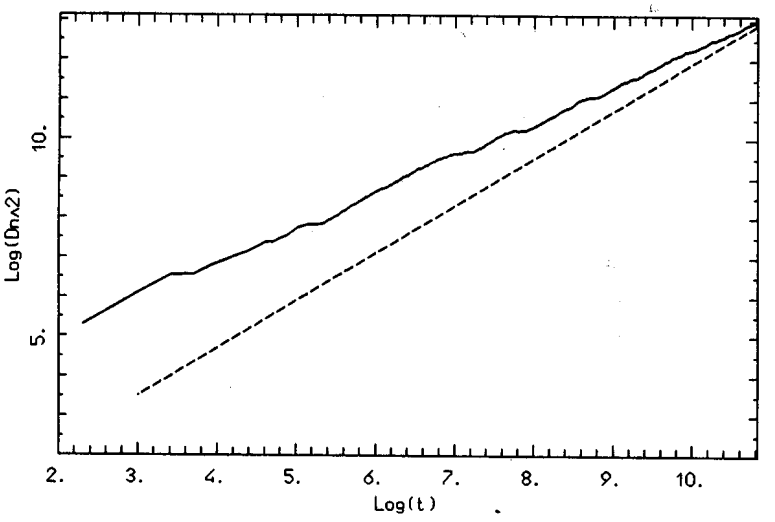

Fig. 5. $\log \sigma_2(t)$ vs. t for $K = L = 5$ $\hbar = 2\pi/(12 + \rho_{\mathrm{GM}})$ (full line). The dashed line has a slope $2D_{\mathrm{H}} = 1.2$.

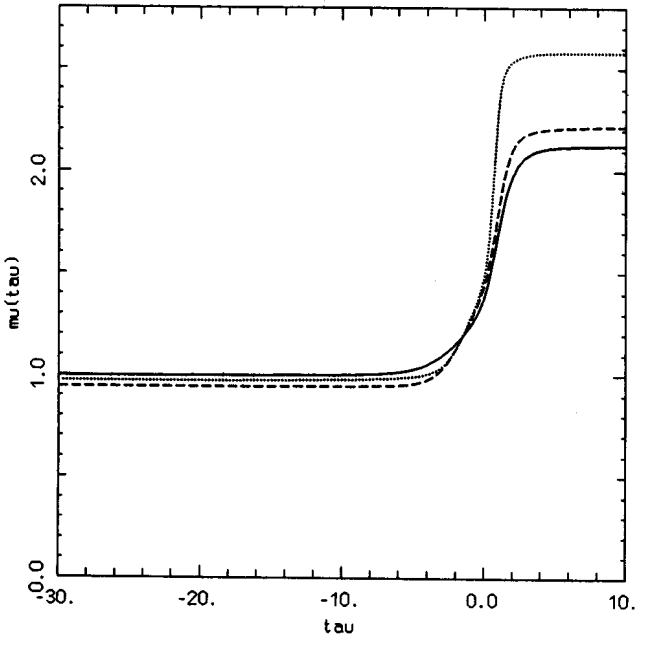

Fig. 6. $\mu(\tau)$ for $K = L = 5$ and different rational approximations to $\hbar = 2\pi/(18 + \rho_{\mathrm{GM}})$ (solid line: $p_n/q_n = 8/157$, dashed line: $p_n/q_n = 13/255$, dotted line: $p_n/q_n = 21/412$).

Table 1. Approximate maximum scaling index for a choice of symmetric parameter values ((*) $\hbar = 2\pi/(6+\rho_{GM})$, (**) $\hbar = 2\pi/(18+\rho_{GM})$).

$K = L = 5$ (**)		$K = L = 5$ (*)		$K = L = 20$ (*)	
p_n/q_n	μ_{max}	p_n/q_n	μ_{max}	p_n/q_n	μ_{max}
1/20	1.55	3/23	2.22	3/23	1.12
2/39	1.89	5/38	2.42	5/38	1.26
3/59	2.04	8/61	2.67	8/61	1.42
5/98	2.00	13/99	2.88	13/99	1.48
8/157	2.13	21/160	2.78	21/160	1.58
13/255	2.22	34/259	2.85	34/259	1.95
21/412	2.58	55/419	3.20	55/419	2.22

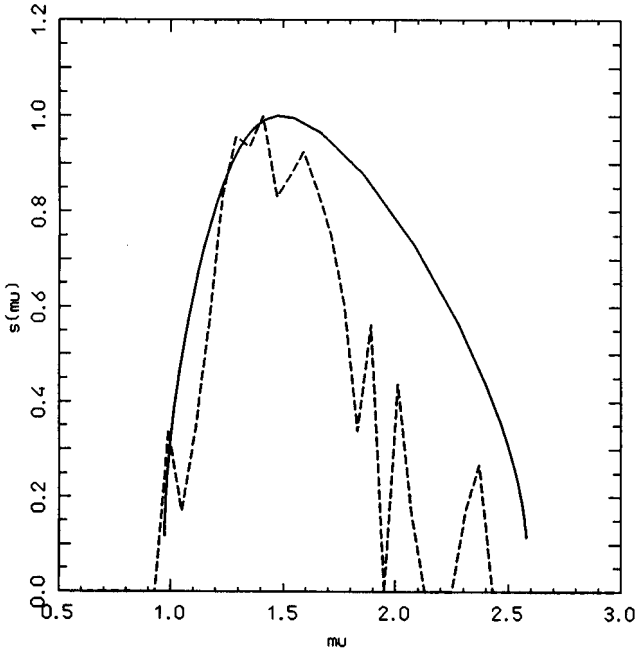

Fig. 7. $s(\mu)$ (dashed line) and its convex envelope (full line) for $K = L = 5$ $\hbar/2\pi = 21/412$.

see Fig. 7. Another dynamical quantity that has been considered in the problem of dynamical localization is the probability distribution over unperturbed states[25,54]: in that case asymptotically one observes an exponentially localized distribution. In Ref. 24 it was pointed out that this distribution function does not possess a

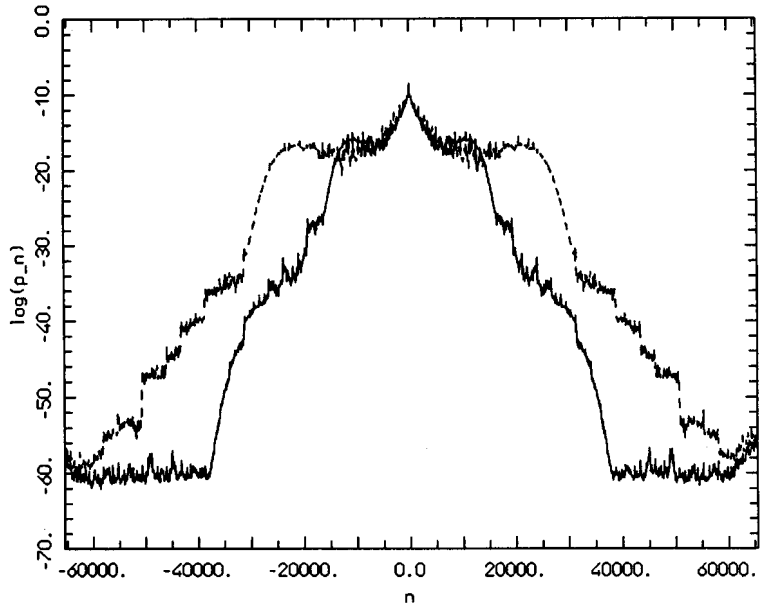

Fig. 8. Probability distribution over unperturbed states $p_t(m)$ ($K = L = 5$ $\hbar = 2\pi/(18 + \rho_{GM})$, solid line: $t = 20000$, dashed line: $t = 40000$).

trivial structure (for instance it is not satisfactorily fitted by a Gaussian distribution): we indeed observed a much structured $p_m(k)$ (see Fig. 8, which refers to the above-mentioned parameters' choice exhibiting enhanced anomalous diffusion). The distribution functions refer to values of the kick number in which the quantum regime has set in since long: another problem is if also for the kicked Harper model a break time is present, up to which the quantum evolution mimics classical dynamics. The existence of an initial transient exhibiting these features was noted in Refs. 24 and 28: in this last paper it was claimed that $t_B \sim \hbar^{-2}$ when the system is classically chaotic. In Fig. 9 the quantum evolution is confronted with classical (normal) diffusion: a coincidence time is clearly present, though by examining a variety of parameters choice we do not have clear evidence for a scaling law exhibited by t_B.

5. Dynamical Exponents and the Phase Diagram

First of all we recall that analogy with unkicked Harper would imply localization (in momentum) for $L < K$, and extended states when $K > L$. We already pointed out that examples were mentioned at variance with such a picture[24,27] and an extended analysis of the global phase diagram[31] confirmed that indeed the situation is rather different. The first attempt was to calculate the momentum growth exponent α from the dynamical evolution of a wavepacket peaked around some initial angular

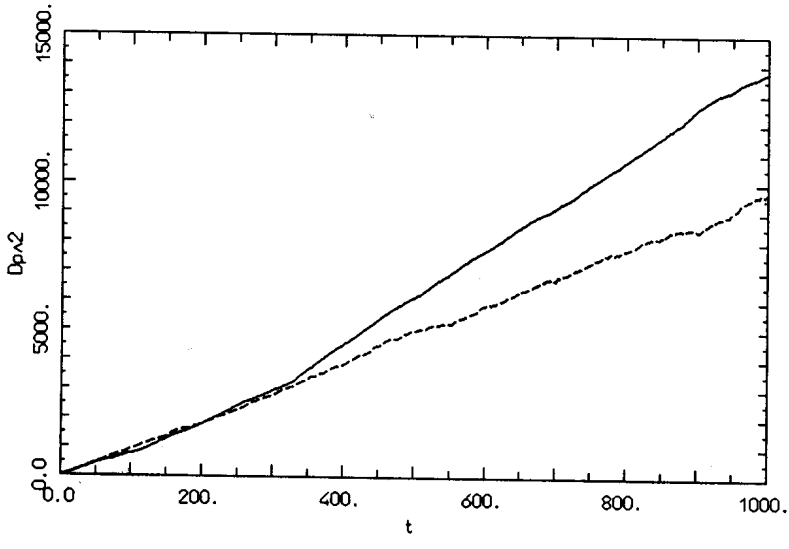

Fig. 9. $\log \sigma_2(t)$ vs. $\log t$ for $K = L = 5$ $\hbar = 2\pi/(18+\rho_{GM})$, the dashed line represents the classical behavior.

momentum value n_0

$$\hbar^2 \frac{1}{T} \sum_{t=1}^{T} \sigma_2(t) = \frac{1}{T} \sum_{t=1}^{T} \hbar^2 \langle n^2(t) \rangle \sim T^{\alpha}$$

where the temporal mean is taken to average out the fluctuations. As illustrated in Fig. 10, a large plethora of exponents ranging from 0 to 2 was found (0 simply means a localized dynamics). Each exponent was obtained by analyzing dynamical time series from $3 \cdot 10^4$ up to 10^6 kicks. We would like to emphasize that such a measure can produce misleading results if one does not look on the overall behavior. To this end very interesting information can be obtained from the study of $\alpha(T)$ at fixed intermediate times T. In fact, in most cases α was found either to converge or to oscillate around some limiting value.

From the same picture it is also clear that no simple transition from localized to extended states can be found (the choice of K/L as x-label does not mean any scaling relation). Nevertheless from this information we can pictorially represent the structure of a phase diagram (see for instance Fig. 11). We would like to point out that the transition line which has been drawn only connects pairs in the parameter space and is not meant to represent a smooth boundary between localized and extended dynamics. Let us then analyze the different regions in the phase plane.

For each fixed L, extremely low values of K indeed correspond to localization (region I), but a transition to unbounded spreading is observed for $K \geq K^*(L)$ well below the critical line ($K = L$) (we call II the region bounded by the critical line and the threshold line ($K = K^*(L)$). In region II we found evidence for

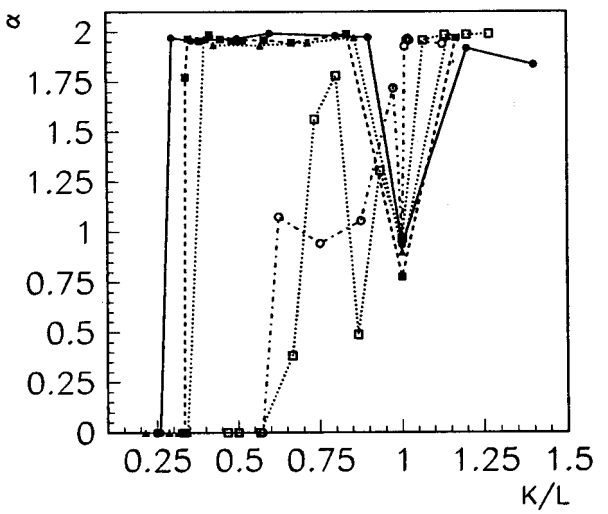

Fig. 10. Dynamical exponent α versus K/L for some fixed L values. Open circles: $L = 3$; open squares: $L = 4$; full circles: $L = 5$; full squares: $L = 6$, full triangles: $L = 7$. Here $\hbar = 2\pi/(6 + \rho_{GM})$.

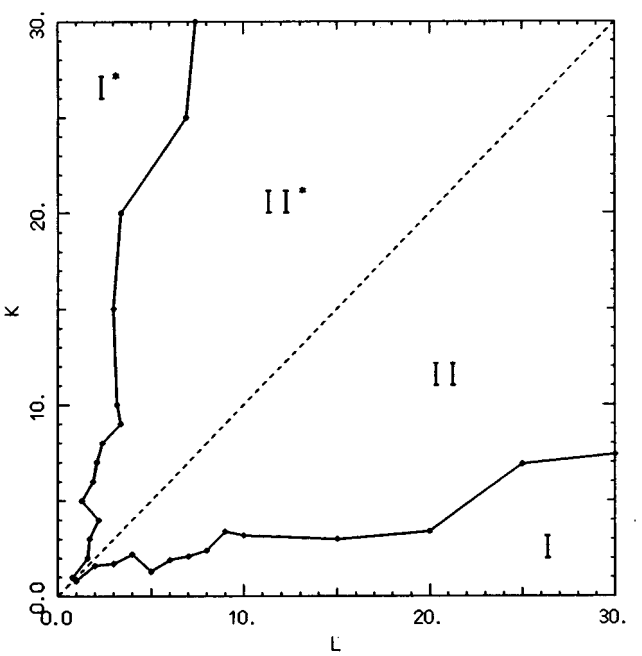

Fig. 11. Phase diagram of the kicked Harper model ($\hbar = 2\pi/(6 + \rho_{GM})$).

the coexistence of pure point and absolutely continuous spectrum (as we shall see this comes from analysis of both correlation decay and thermodynamics). The remaining part of the phase diagram is determined by duality (we already commented upon the self-dual critical line $K = L$): region I* presents a purely continuous spectrum, while in II* we still have evidences of a mixed spectrum (* means region obtained as image according to the transformation $K \mapsto L \quad L \mapsto K$). We remark again that we do not have enough information on very small scales to check whether the threshold line is smooth or not.

To illustrate the behavior in different regions we first consider parameter pairs belonging to regions II and II*. We first notice (Fig. 12) that unbounded spreading is evident in both cases (with an exponent extremely near to $\chi = 2$, i.e. ballistic propagation). We also checked, for a set of other moments, whether the moments' scaling law shows anomalies[55]: that is if we put (cfr. (2.4)) $\sigma_q(m) \simeq m^{\phi(q)}$ we essentially control whether $\phi(q)$ is given by a straight line (whose slope is $\chi/2$) or some sort of crossover between different regimes determines a non trivial form of $\phi(q)$. Within numerical errors we do not have evidence (in these cases as well in all other cases examined) of deviations from a straight line behavior of $\phi(q)$. Correspondingly to unbounded propagation we also observe an expanding form for $p_m(k)$ (see Fig. 13, notice that near the origin still a "localization" peak persists), suggesting that the unperturbed basis is being filled linearly in time. These features indicate the presence in the spectrum of a continuous component (we remark that rigorously this is guaranteed only if the spreading is ballistic[56]).

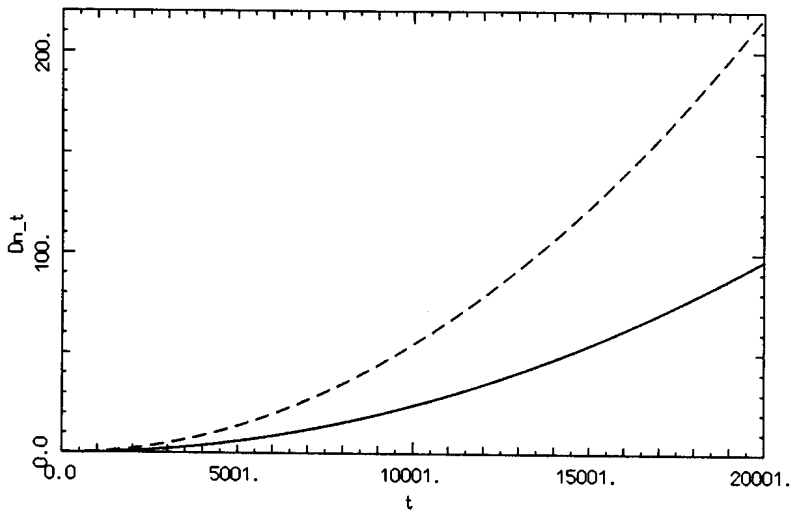

Fig. 12. $\sigma_2(t)$ vs. t for $K = 4$ $L = 7$ (full line) (II) and $K = 7$ $L = 4$ (dashed line) (II*): $\hbar = 2\pi/(6 + \rho_{GM})$. Units along the vertical axis are arbitrary.

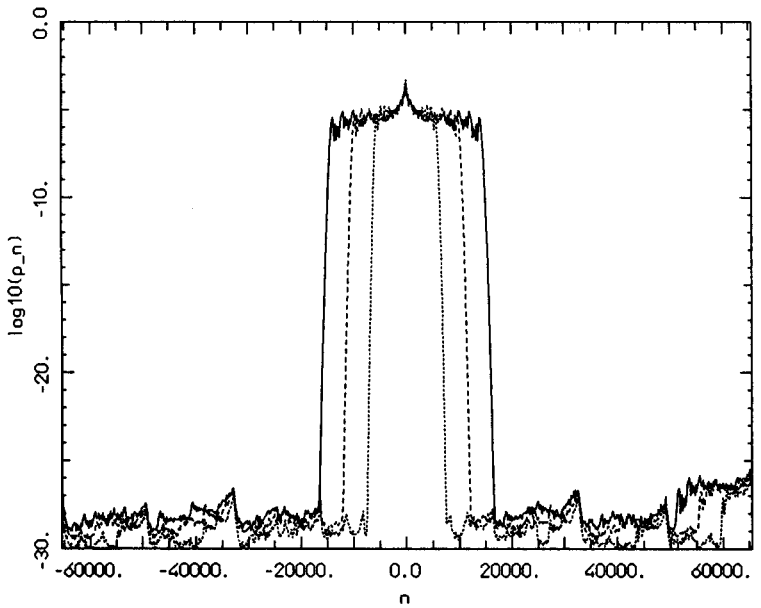

Fig. 13. Probability distribution over unperturbed states $p_t(m)$ ($K = 4$ $L = 5$ $\hbar = 2\pi/(6 + \rho_{GM})$ (II); dotted line: $t = 8000$, dashed line: $t = 14000$, full line: $t = 20000$). In the conjugate region $p_t(m)$ exhibits the same features.

Conversely the behavior of correlation functions (see Fig. 14) strongly suggests the presence of a pure point component in the spectrum, as $C_{\text{int}}(m)$ does not seem to tend to zero (but to a finite limit) in the $m \to \infty$ limit. The convergence to the asymptotic limit seems ruled by a power-law, thus this limit is not easily estimated[57] without further information, (see Ref. 42). This is consistent with thermodynamic analysis of the spectrum: in Table 2 we report on $\mu_{\min}$ (which seems well defined) and $\mu_{\max}$ calculations for periodic approximations: the $\{\mu_{\max}\}$ sequence reveals the presence of bandwidths shrinking faster than exponentially, which, according to the arguments in the former sections, is the thermodynamic signal for a pure point component. The coexistence of two different contributions to the thermodynamic functions is also evident from evaluation of different orders of the scaling spectrum (Fig. 15).

A completely different situation appears when we consider dual parameter pairs in region I and I*. As regards spreading of the wave packet they exhibit, respectively, dynamical localization and (ballistic) unbounded spreading (see Fig. 16). This behavior is as usually reflected in snapshot pictures of probability distributions over unperturbed states: they indicate dynamical localization in region I and linear in time spreading over the unperturbed basis in region I* (Fig. 17). This indicates that in I we have pure point spectrum, while in the dual conjugate region I* the spectrum is entirely continuous. This is confirmed by the behavior of $C_{\text{int}}(m)$,

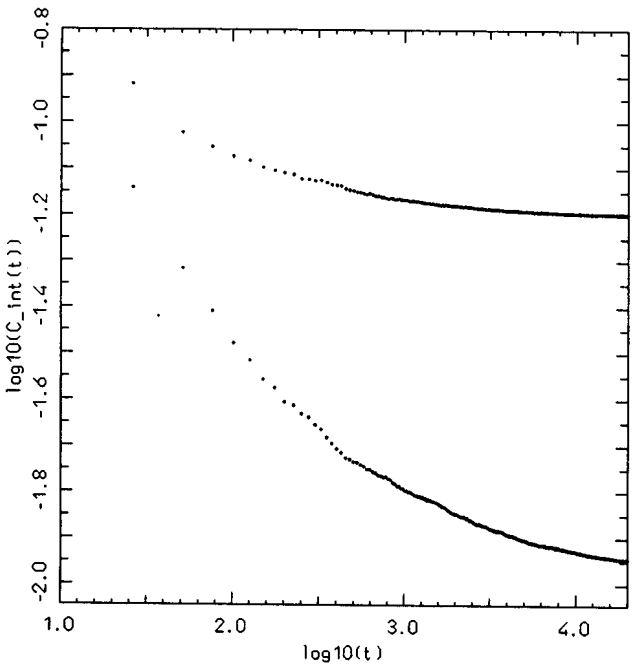

Fig. 14. $\log C_{\rm int}(t)$ vs. $\log t$ (upper points: $K = 4$ $L = 7$ $\hbar = 2\pi/(6 + \rho_{\rm GM})$ (II), lower points: $K = 7$ $L = 4$ $\hbar = 2\pi/(6 + \rho_{\rm GM})$ (II*)).

Table 2. Approximate minimum and maximum scaling indices some rational approximation to $(\hbar = 2\pi/(6 + \rho_{\rm GM}))$ for $K = 7$ $L = 4$.

p_n/q_n	$\mu_{\rm min}$	$\mu_{\rm max}$
2/15	1.13	1.86
5/38	1.06	2.55
13/99	1.02	4.20
34/259	1.02	5.05

which in region I* decays to zero, according to a power-law (see Fig. 18). We have to remark that the decay exponent in this region does not seem to be universal, in contrast to what claimed in.[29,b] Pure point character of the spectrum is confirmed by thermodynamic analysis: while in region I lack of good scaling is exhibited by all scaling spectrum, in region I* we observe good convergence, without any high μ unstable phase (see Fig. 19 and Table 3).

[b]The relation $\delta = D_2$ (Ref. 29) seems, however, satisfied.[42,53]

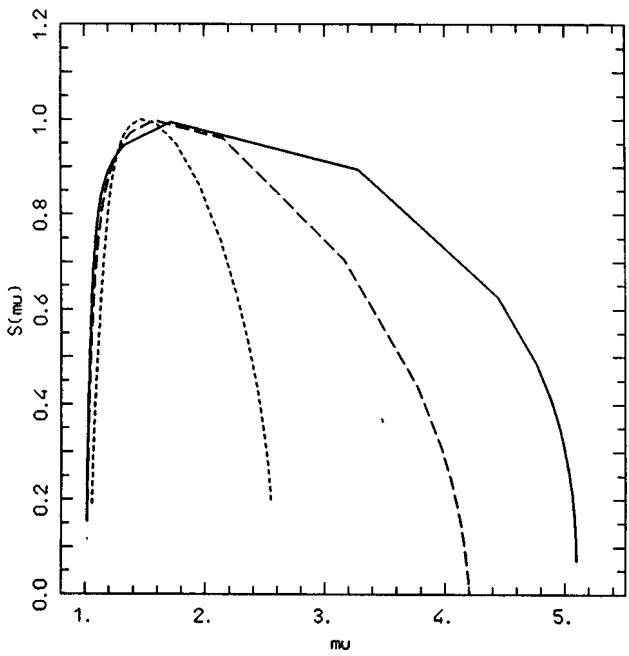

Fig. 15. $S(\mu)$ for $K = 7$ $L = 4$ and different approximations to $\hbar = 2\pi/(6 + \rho_{GM})$: dotted line: $p_n/q_n = 5/38$, dashed line: $p_n/q_n = 13/99$, full line: $p_n/q_n = 34/259$.

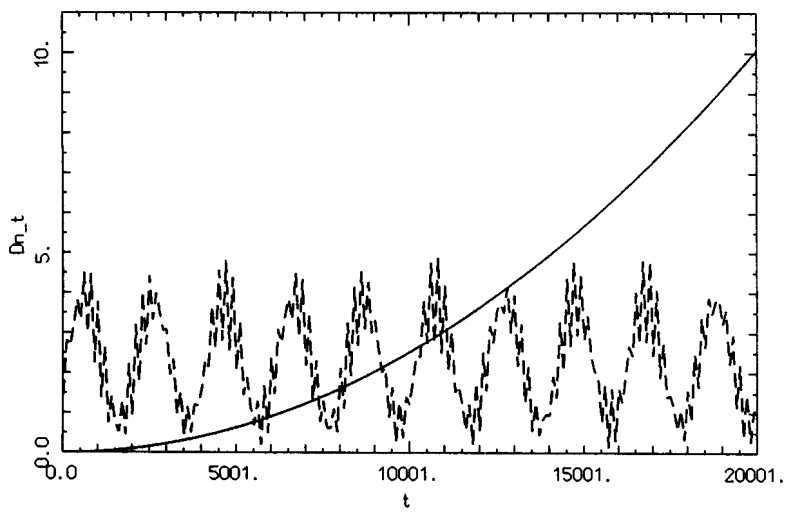

Fig. 16. $\sigma_2(t)$ vs. t for $K = 4$ $L = 2$ (full line) (I*) and $K = 2$ $L = 4$ (dashed line) (I), $\hbar = 2\pi/(6 + \rho_{GM})$. For the full line each vertical unit corresponds to $1.5 \cdot 10^7$.

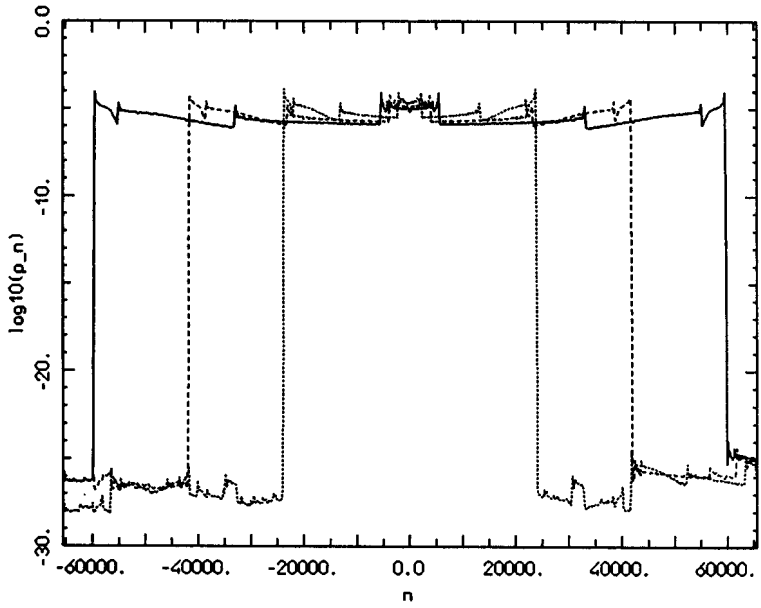

Fig. 17. Probability distribution over unperturbed states $p_t(m)$ ($K = 2.5$ $L = 0.5$ $\hbar = 2\pi/(6+\rho_{GM})$ (I*); dotted line: $t = 8000$, dashed line: $t = 14000$, full line: $t = 20000$).

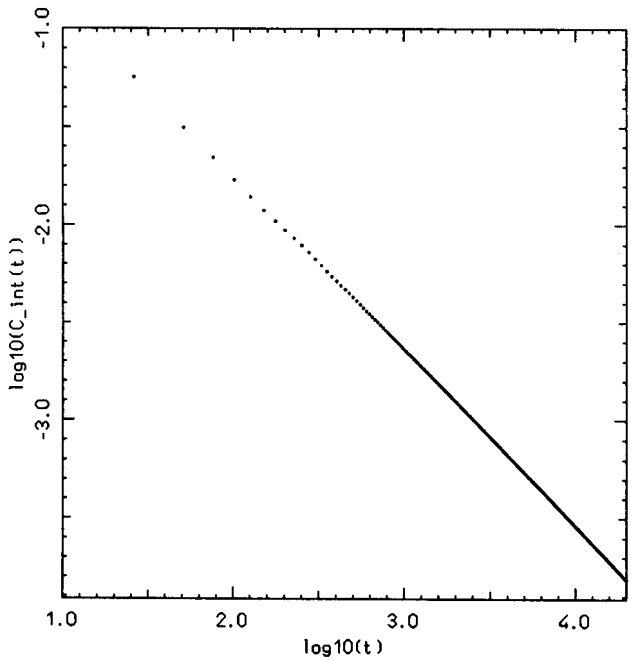

Fig. 18. $\log C_{\rm int}(t)$ vs. t for $K = 4$ $L = 2$ $\hbar = 2\pi/(6 + \rho_{GM})$ (I*).

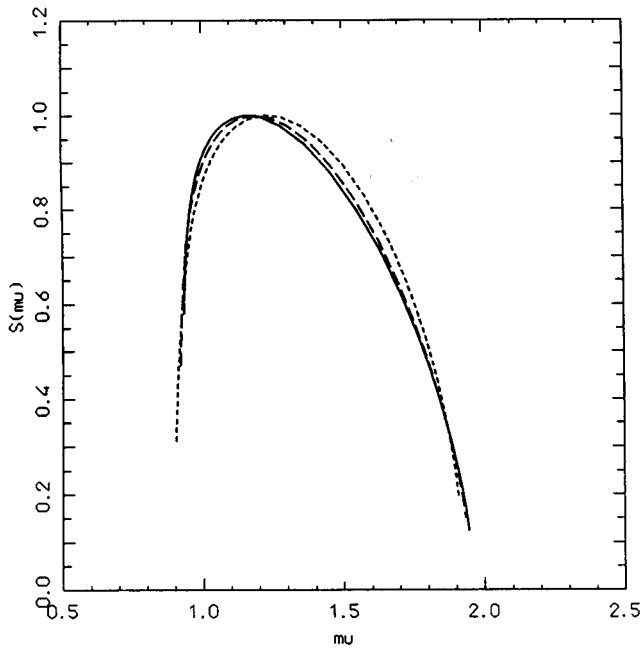

Fig. 19. $S(\mu)$ for $K = 4$ $L = 2$ and different approximations to $\hbar = 2\pi/(6 + \rho_{GM})$: dotted line: $p_n/q_n = 5/38$, dashed line: $p_n/q_n = 13/99$, full line: $p_n/q_n = 34/259$.

Table 3. Approximate minimum and maximum scaling indices some rational approximation to $(\hbar = 2\pi/(6 + \rho_{GM}))$ for $K = 4$ $L = 2$.

p_n/q_n	μ_{min}	μ_{max}
2/15	.91	1.87
3/23	.90	1.94
5/38	.90	1.91
8/61	.92	1.92
13/99	.92	1.93
21/160	.93	1.94
34/259	.93	1.95
55/419	.94	1.95

6. Exact Results on the Kicked Harper Model

The dynamical behavior of any quantum model is strictly connected with its spectral properties. It is well-known for example that the presence of a continuous compo-

nent in the spectrum leads to an unbounded propagation. A more involved situation is connected with the quantum diffusive motion: in fact it has been proved[18] that such a situation can only be accomplished by the presence of a singular spectrum.

The presence of ballistic propagation was found in closely-related kicked systems, e.g. the kicked rotator,[58] the kicked harmonic oscillator,[59] and is usually related with the rationality of the relevant frequency ratios of the system. For this reason this situation is usually called quantum resonance. Since the rationality is often related with some periodicity of the system, the same result can also be stated as the invariance of the evolution operator under the action of some group of translations in the relevant space. In this case, in fact, due to the Bloch theorem, the presence of a continuous component in the spectrum is insured together with the unbounded diffusion of quantum states. A key to the theoretical analysis of the KH model is obtained by investigating the same model "on the line", i.e. taking the variable θ in Eq. (2.1) on the whole line rather in $(0, 2\pi)$. The quantum model is in this case described by the propagator

$$\hat{U}(L, K) = \exp\left(-i\frac{L}{\hbar}F(\hat{p})\right)\exp\left(-i\frac{K}{\hbar}F(\hat{x})\right) = \hat{U}^{\dagger}(-K, -L) \tag{6.1}$$

where F is a 2π-periodic, real even function. In the KH case $F(x) = \cos(x)$ but the results of this section hold for a larger class of potentials.[34] How is the model "on the line" related to the conventional model "on the circle"? In the classical case the phase space is the (x, p) plane in the former case, and the cylinder (θ, p) in the latter: orbits on the cylinder are trivially obtained by folding orbits in the plane. In the quantum case, an equivalent to classical folding is provided by Bloch's theorem. Indeed, due to the periodicity of F, any wavefunction $\psi(x)$ can be written as a superposition of 2π-periodic functions $\psi_\eta(x)$

$$\psi(x) = C\int_0^1 d\eta e^{i\eta x}\psi_\eta(x) \tag{6.2}$$

where C is a normalizing constant and $\psi_\eta(x)$ is the same function at fixed quasi-momentum η. From the mathematical standpoint the decomposition (6.2) defines a fibration of the Hilbert space. Then the action of the evolution operator over a generic wavefunction can be represented as

$$\hat{U}(L, K)\psi(x) = C\int_0^1 d\eta e^{i\eta x}\hat{U}_\eta(L, K)\psi_\eta(x) \tag{6.3}$$

where the "fibre map" is given by

$$\hat{U}_\eta(L, K) = \exp\left(-i\frac{L}{\hbar}F(\hbar(\hat{n} + \eta))\right)\exp\left(-i\frac{K}{\hbar}F(\hat{x})\right)$$

and $\hat{n} = -i\partial/\partial\theta$.

The operators $\hat{U}_\eta(L, K)$ at different η define different (and non-equivalent) quantizations of the KH model "on the circle", and their spectral properties are strictly related with those of the operator (6.1).[34]

A quite similar Bloch decomposition can be obtained by exploiting the p-periodicity instead of the x-one. A new family of fibre maps are obtained in this way. The duality property of the KH model can be simply stated as the spectral equivalence of x-fibre maps $\hat{U}_\eta(L, K)$ with p-fibre maps $\hat{U}_\eta(K, L)$. On such grounds the following theorem can be proved:

Theorem

For almost all $L \in \mathbb{R}$ one of the following properties is true:

i) $\hat{U}_\eta(L, 1)$ has a non-empty continuous spectrum for almost all η;
ii) $\hat{U}_\eta(1, L)$ has a non-empty continuous spectrum for almost all η;
iii) both $\hat{U}_\eta(L, 1)$ and $\hat{U}_\eta(1, L)$ have a non-empty continuous spectrum for almost all η.

In particular $\hat{U}_\eta(1, 1)$ is found to have a non-empty continuous spectrum for almost all η.

In Ref. 34 this theorem (Theorem 2) was stated for almost all $L \leq 0$ (note the different signs in the definition of the evolution operator); nevertheless it can be easily generalized to $L > 0$.

We stress here that this theorem holds for a generic choice of the potential in a class of periodic analytic functions (for the explicit construction of such a set see the Appendix 1 of Ref. 34). It is then clear that such a theorem provides an interpretation, even if partial, of the phase diagram introduced in Sec. 5.

The apparently strange behavior observed in Ref. 27 namely a ballistic propagation for two conjugate pairs of parameters (K, L), (L, K) was then numerically analyzed by using the full operator (6.1). An initial coherent state has been decomposed in $N_p = 128$ fibres, each of one was iterated, under the fibre map, for $t = 400$ kicks. All these fibres were then put together to reconstruct the state at time t and the related Husimi function $h(q, p, t) = |\langle z|\psi(t)\rangle|^2$ z being the coherent state peaked at $q + ip$. A phase space portrait of the Husimi function is shown in Figs. 20, 21 and 22. The first two pictures refer to the conjugate pairs of parameters while, for sake of comparison, we plot in Fig. 22 the Husimi function for $K = L$ (diffusive propagation). As one can see the ballistic propagation is characterized by a spread along orthogonal chimneys (in such a way that $\Delta p^2 \sim \Delta q^2 \sim t^2$). This explains why interchanging K with L, namely changing p with q the same behavior is obtained. In Fig. 22 the spread fills all the phase space with $\Delta p^2 \sim \Delta q^2 \sim t$). It is interesting to remark that these three types of propagation are consistent with a linear growth of the phase space area, which represents the semiclassical number of states.

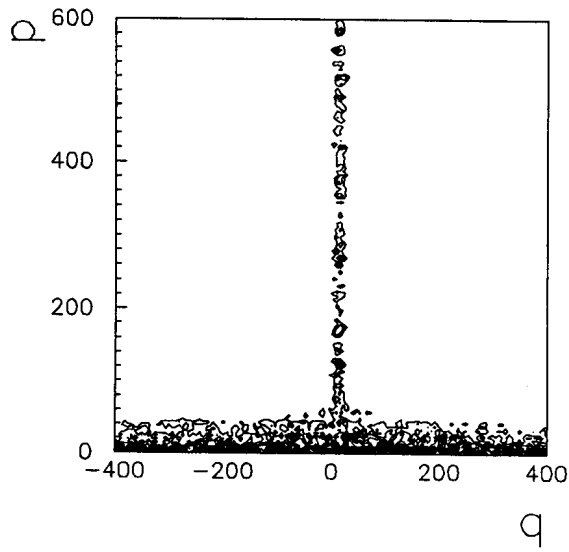

Fig. 20. Contour plot of the Husimi function after 400 kicks for $K = 3.1$, $L = 6$, $\hbar = 2\pi/(6+\rho_{GM})$. The initial coherent state was peaked in (10, 10).

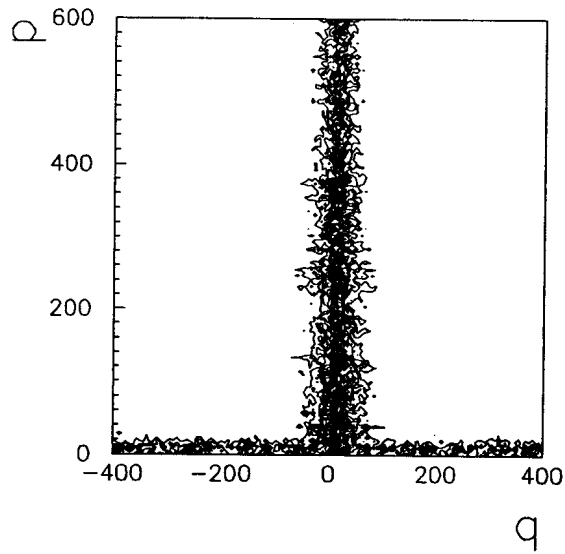

Fig. 21. The same as Fig. 20 with K and L interchanged.

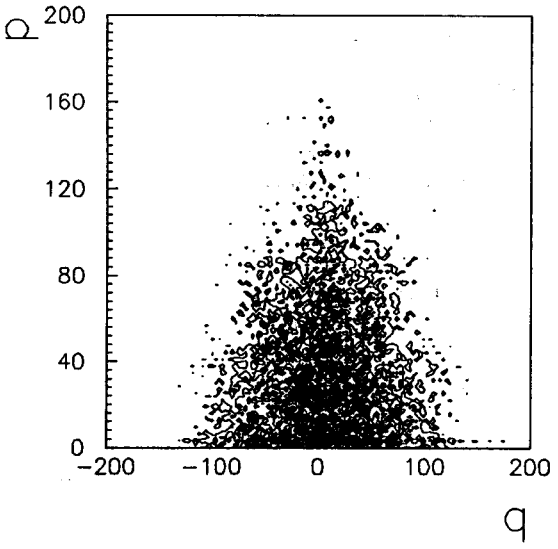

Fig. 22. The same as Fig. 20 with $K = L = 5$.

7. Conclusion

We have presented a number of results describing in some detail the behavior of the kicked Harper model. We have given evidence of its rich phase diagram structure, which strongly contrasts with either what would be expected on the grounds of the usual Harper's equation or with the paradigm of quantum dynamical localization, which has been one of the guiding principles in the discipline of quantum chaos. The analysis has been carried through both by dynamical investigations (spreading of the wave function, decay of temporal autocorrelation functions) and by means of the thermodynamic formalism. Obviously the classical map we started from has peculiarities which make it quite different from the standard map (which is the classical counterpart of the quantum kicked rotator); we believe here lies the major problem to be solved, i.e. to understand what features of classical dynamics lead to quantum localization or diffusion (at least at the semiclassical level).

References

1. P. G. Harper, *Proc. Phys. Soc.* **A68**, 874 (1955).
2. J. Bellissard and A. Barelli, *J. Phys. I France* **3**, 471 (1993); J. Bellissard in *From Number Theory to Physics*, eds. M. Waldschmidt, P. Moussa, J.-M. Luck and C. Itzykson (Springer, Berlin, 1992).
3. P. A. Lee, T. M. Rice and P. W. Anderson, *Solid State Commun.* **14**, 703 (1974); P. Bak, *Rep. Progr. Phys.* **45**, 587 (1982); S. Alexander, *Phys. Rev.* **B27**, 1541 (1983); R. Rammal, T. C. Lubensky and G. Toulouse, *Phys. Rev.* **B27**, 2820 (1983); J. B. Sokoloff, *Phys. Rep.* **126**, 189 (1985).

4. D. J. Thouless, M. Kohmoto, M. P. Nightingale and M. den Nijs, *Phys. Rev. Lett.* **49**, 405 (1982); D. J. Thouless, in *Number Theory and Physics*, eds. J.-M. Luck, P. Moussa and M. Waldschmidt (Springer, Berlin, 1990).
5. M. Ya. Azbel, *JETP* **19**, 634 (1964).
6. S. Aubry and G. André, *Ann. Israel Phys. Soc.* **3**, 133 (1980).
7. D. J. Thouless, *J. Phys.* **C5**, 77 (1972).
8. L. Pastur and A. Figotin, *Spectra of Random and Quasiperiodic Operators*, (Springer, Berlin, 1992).
9. H. L. Cycon, R. G. Froese, W. Kirsch and B. Simon, *Schrödinger Operators* (Springer, Berlin, 1987).
10. J. Avron and B. Simon, *J. Funct. Anal.* **43**, 1 (1981).
11. M. Kohmoto, *Phys. Rev. Lett.* **51**, 1198 (1983); C. Tang and M. Kohmoto, *Phys. Rev.* **B34**, 2041 (1986).
12. H. Hiramoto and M. Kohmoto, *Int. J. Mod. Phys.* **B6**, 281 (1992).
13. H. Hiramoto and S. Abe, *J. Phys. Soc. Jap.* **57**, 1365 (1988).
14. H. Hiramoto and S. Abe, *J. Phys. Soc. Jap.* **57**, 230 (1988).
15. T. Geisel, R. Ketzmerick and G. Petschel, *Phys. Rev. Lett.* **66**, 1651 (1991).
16. T. Geisel, R. Ketzmerick and G. Petschel, in *Quantum Chaos — Quantum Measurement*, eds. P. Cvitanović, I. C. Percival and A. Wirzba (Kluwer, Dordrecht, 1992).
17. K. Machida and M. Fujita, *Phys. Rev.* **B34**, 7367 (1986).
18. I. Guarneri, *Europhys.Lett.* **10**, 95 (1989); **21**, 729 (1993).
19. J.-M. Combes, "Connections between quantum dynamics and spectral properties of time–evolution operators", Marseille preprint, 1992.
20. R. B. Stinchcombe and S. C. Bell, *J. Phys.* **A20**, L739 (1987); S. C. Bell and R. B. Stinchcombe, *J. Phys.* **A22**, 717 (1989).
21. D. R. Hofstadter, *Phys. Rev.* **B14**, 2239 (1976).
22. R. A. Pasmanter, *Phys. Rev.* **A42**, 3622 (1990).
23. P. Leboeuf, J. Kurchan, M. Feingold and D. P. Arovas, *Phys. Rev. Lett.* **65**, 3076 (1990); *Chaos* **2**, 125 (1992).
24. R. Lima and D. Shepelyansky, *Phys. Rev. Lett.* **67**, 1377 (1991).
25. G. Casati, B. V. Chirikov, J. Ford and F. M. Izrailev, in *Stochastic Behavior in Classical and Quantum Hamiltonian Systems*, eds. G. Casati and J. Ford, *Lecture Notes in Physics* **93** (Springer, Berlin, 1979); F. M. Izrailev, *Phys. Rep.* **196**, 299 (1990); G. Casati and L. Molinari, *Progr. Theor. Phys. Suppl.* **98**, 287 (1989); B. V. Chirikov, in *Chaos and Quantum Physics*, eds. M.-J. Giannoni, A. Voros and J. Zinn-Justin (North-Holland, Amsterdam, 1991).
26. G. M. Zaslavsky, M. Yu. Zakharov, R. Z. Sagdeev, D. A. Usikov and A. A. Chernikov, *JETP Lett.* **44**, 451 (1986); V. V. Afanasiev, A. A. Chernikov, R. Z. Sagdeev and G. M. Zaslavsky, *Phys. Lett.* **A144**, 229 (1990); R. Z. Sagdeev, D. A. Usikov and G. M. Zaslavsky, *Nonlinear Physics* (Harwood, Chur, 1988).
27. D. Shepelyansky, in *Quantum Chaos – Theory and Experiment* (see Ref. 17).
28. T. Geisel, R. Ketzmerick and G. Petschel, *Phys. Rev. Lett.* **67**, 3635 (1991).
29. R. Ketzmerick, G. Petschel and T. Geisel, *Phys. Rev. Lett.* **69**, 695 (1992).
30. R. Artuso, G. Casati and D. Shepelyansky, *Phys. Rev. Lett.* **68**, 3826 (1992).
31. R. Artuso, F. Borgonovi, I. Guarneri, L. Rebuzzini and G. Casati, *Phys. Rev. Lett.* **69**, 3302 (1992).
32. R. Artuso and G. Casati, "Thermodynamic formalism of quasienergy spectra", in *Proceedings of the Workshop "From Classical to Quantum Chaos"*, to be published.
33. J. Bellissard and A. Barelli, in *Quantum Chaos – Quantum Measurement* (see Ref. 17).
34. I. Guarneri and F. Borgonovi, *J. Phys.* **A26**, 119 (1993).

35. D. Wei and D. P. Arovas, *Phys. Lett.* **A158**, 469 (1991).
36. J. C. Kimball, V. A. Singh and M. D'Souza, *Phys. Rev.* **A45**, 7065 (1992).
37. J. M. Greene, *J. Math. Phys.* **20**, 1183 (1979); R. S. MacKay, *Physica* **D7**, 283 (1983); R. S. MacKay, J. D. Meiss and I. C. Percival, *Physica* **D13**, 55 (1984).
38. S.-J. Chang and K.-J. Shi, *Phys. Rev.* **A34**, 7 (1986).
39. J. Bellissard, in *Trends and Developments in the Eighties*, eds. S. Albeverio and Ph. Blanchard (World Scientific, Singapore, 1985).
40. B. Sutherland, *Phys. Rev. Lett.* **57**, 770 (1986).
41. T. Dittrich and U. Smilansky, *Nonlinearity* **4**, 59; 85 (1991).
42. D. Belluzzo, Thesis (Universitá degli Studi di Milano, 1993); R. Artuso, D. Belluzzo and G. Casati, " Thermodynamic analysis of the spectral measure of kicked quantum systems", preprint, Universitá di Milano, Sede di Como, 1993; the approach was stimulated by some considerations in M. Samuelides, R. Fleckinger, L. Touzillier and J. Bellissard, *Europhys. Lett.* **1**, 203 (1986).
43. J. W. S. Cassels, *An Introduction to Diophantine Approximation* (Cambridge Univ. Press, Cambridge, 1957); I. Niven, *Irrational Numbers* (Wiley, New York, 1963).
44. A. Y. Khinchin, *Continued Fractions*, (Univ. of Chicago Press, Chicago, 1964).
45. R. Bowen, "Equilibrium states and the ergodic theory of Anosov diffeomorphism", *Lect. Notes in Math.* **470** (Springer, Berlin, 1975); D. Ruelle, *Thermodynamic Formalism* (Addison–Wesley, Reading, 1978); E. B. Vul, Ya. G. Sinai and K. M. Khanin, *Russ. Math. Surv.* **39**, 1 (1984); R. Benzi, G. Paladin, G. Parisi and A. Vulpiani, *J. Phys.* **A17**, 3521 (1984); T. C. Halsey, M. H. Jensen, L. P. Kadanoff, I. Procaccia and B. I. Shraiman, *Phys. Rev.* **A107**, 1141 (1986); M. J. Feigenbaum, *J. Stat. Phys.* **46**, 919; 925 (1987).
46. R. Artuso, P. Cvitanović and B. G. Kenny, *Phys. Rev.* **A39**, 268 (1989).
47. J.-P. Eckmann and D. Ruelle, *Rev. Mod. Phys.* **57**, 617 (1980) and references therein.
48. P. Cvitanović, in *Non-linear Evolution and Chaotic Phenomena*, eds. P. Zweifel, G. Gallavotti and M. Anile (Plenum, New York, 1987).
49. H. G. E. Hentschel and I. Procaccia, *Physica* **D8**, 435 (1983).
50. B. Dorizzi, B. Grammaticos and Y. Pomeau, *J. Stat. Phys.* **37**, 93 (1984); D. Shepelyansky, *Physica* **D28**, 103 (1987).
51. M. Kohmoto, *J. Phys. Soc. Jap.* **60**, 2876 (1991).
52. R. Artuso, E. Aurell and P. Cvitanović, *Nonlinearity* **3**, 361 (1990).
53. I. Guarneri and G. Mantica, "On the asymptotic properties of quantum dynamics in the presence of a fractal spectrum", preprint (Universitá di Milano, Sede di Como, 1993).
54. B. V. Chirikov, F. M. Izrailev and D. L. Shepelyansky, *Sov. Sci. Rev.* **C2**, 209 (1981).
55. T. Geisel and J. Nierwetberg, *Z. Phys.* **B56**, 59 (1984); I. S. Aranson, M. I. Rabinovich and L. S. Tsimring, *Phys. Lett.* **A125**, 523 (1990); L. S. Tsimring, *Physica* **D63**, 41 (1993).
56. B. Simon, *Comm. Math. Phys.* **134**, 209 (1990).
57. D. Levin, *J. Comput. Math. Sect.* **B3**, 371 (1973); N. Osada, *SIAM J. Numer. Anal.* **27**, 178 (1990); R. Artuso, *J. Phys.* **A21**, L923 (1988).
58. F. Izrailev and D. Shepelyansky, *Theor. Mat. Fiz.*, **43**, 417 (1980).
59. F. Borgonovi and L. Rebuzzini, "Translational invariance in the kicked harmonic oscillator", preprint FNT/T-92/19 (Università di Pavia, 1992), submitted to *Nonlinearity*.